Study of JT-60SA Operation Scenario using a Plasma Equilibrium Control Simulator*)

Yoshiaki MIYATA, Takahiro SUZUKI, Shunsuke IDE, Hajime URANO and Takaaki FUJITA

Japan Atomic Energy Agency, 801-1 Mukoyama, Naka, Ibaraki 311-0193, Japan

(Received 7 December 2012 / Accepted 19 May 2013)

A plasma equilibrium control simulator has been developed to simulate the control of plasma position and shape as well as plasma current I_P. The simulator consists of an equilibrium calculation component and a controller component. The plasma position, shape, and I_P are obtained as a result of an equilibrium calculation under the specified poloidal field coil current. The control simulator enables simulation of the control of the position, shape, and I_P using the isoflux technique, and it optimizes the control logic of the coil current in JT-60SA. The plasma equilibrium control is simulated during I_P ramp-up. The controllability of the last closed flux surface is also validated during I_P flat-top.

Keywords: JT-60SA, plasma equilibrium, control logic, poloidal field coil, isoflux

DOI: 10.1585/pfr.8.2405109

1. Introduction

The precise control of plasma position is a key issue in safe and stable plasma operation of JT-60SA [1, 2], ITER, and DEMO. Simulation of the control of plasma equilibrium such as position, shape, and I_P in JT-60SA is being studied to predict the controllability of the ITER and DEMO [3, 4] plasmas. Studies of the control of the plasma equilibrium for JT-60SA will contribute to a control scheme and suitable operation regimes for ITER and DEMO.

The free plasma boundary time varying codes MAXFEA, PET, and DINA [5] were used to analyze the non-linear performance of the controllers. Studies with these codes have demonstrated the required performance of the ITER poloidal field (PF) coil system. Several studies have been carried out to estimate the effect of the conducting structures on the plasma position and shape as well as plasma currentI_P. Details of the model of the conducting structures become more important when the stability margin decreases.

The JT-60SA device is capable of confining high-temperature plasma lasting longer than the time scales that characterize key plasma processes. There are 10 PF coils and 2 fast plasma position control (FPPC) coils. The PF coils and FPPC coils are superconducting and in-vessel copper coils, respectively. The PF coils consist of 4 central solenoid (CS) modules and 6 equilibrium field (EF) coils. The feedback controller regulates the currents of the PF and FPPC coils in reference to the I_P measured by a Rogowski coil, and the plasma position and shape are reproduced by the Cauchy condition surface (CCS) method [6]. Advanced control logic for the PF coils and in-vessel coils is necessary because the magnetic field for plasma control cannot be produced solely by each PF coil and FPPC coil in JT-60SA.

A plasma position and shape control simulator that incorporates the effect of eddy currents has been developed in order to study the techniques of plasma position and shape control in JT-60SA [7]. A function that calculates the self-consistent I_P with flux consumption was incorporated into the position and shape control simulator. With this new system, it is possible to simulate the control of plasma position, shape, and I_P using the isoflux [8] technique and optimize the control logic of the coil current in the JT-60SA.

2. Outline of the Control Simulator

The plasma equilibrium control simulator consists of an equilibrium calculation component and a controller component. A function that calculates the self-consistent I_P with flux consumption has been incorporated into the equilibrium calculation component in order to simulate I_P control. Figure 1 shows the calculation flow of the plasma equilibrium control simulator. In the equilibrium calculation component of the simulator, the plasma position, shape and I_P are obtained as a result of an equilibrium calculation. There are 4 calculation steps in the equilibrium calculation. Step 1, Step 2 and Step 3 were established in the previous plasma position and shape control simulator, and Step 4 has been added for the control of I_P. After finishing the calculation from Steps 1 to 3, the plasma position and shape are obtained under the given coil current. At Step 4, the self-consistent I_P with flux consumption is calculated in reference to the equilibrium obtained from

author's e-mail: miyata.yoshiaki@jaea.go.jp

*) This article is based on the presentation at the 22nd International Toki Conference (ITC22).

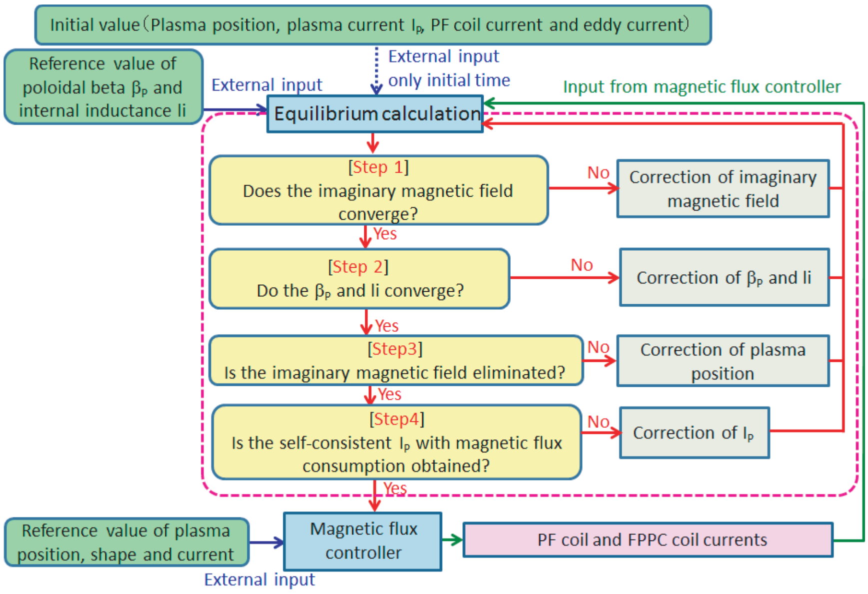

Fig. 1 Calculation flow of the control simulator. It consists of an equilibrium calculation component and a controller component.

Step 1 to 3.

The function that controls the I_P has been incorporated into the controller component in order to simulate I_P control. The controller receives the reference values and actual values of plasma position, shape, and I_P. It modifies the PF and FPPC coil currents to reduce the difference between the reference values and actual values. At the next time step, the equilibrium calculation receives the modified coil current and reference values of the poloidal beta β_P and internal inductance l_i. By iterating these procedures, feedback control of plasma position, shape, and I_P by controlling the coil current is simulated.

2.1 Calculation of I_P with flux consumption

The I_P with the flux consumption is calculated at Step 4 in Fig. 1. The magnetic flux Ψ_{op} required for the inductive operation is defined by:

$$\Psi_{op} = \Psi_{ramp} + \Psi_{flat\text{-}top}, \tag{1}$$

where Ψ_{ramp} is the magnetic flux required for the I_P ramp-up, and $\Psi_{flat\text{-}top}$ is the magnetic flux required for the current drive by inductive operation. The units of the variables Ψ_{op}, Ψ_{ramp}, and $\Psi_{flat\text{-}top}$ are in webers (Wb). The I_P ramp-up is provided by the magnetic flux swing of the CS coils. The required Ψ_{ramp} is defined by:

$$\Psi_{ramp} = L_P I_P + C_{Ejima}\mu_0 R_P I_P, \tag{2}$$

where L_P is the plasma self-inductance, I_P is the plasma current, R_P is the plasma major radius, C_{Ejima} (= 0.45) is the Ejima coefficient, and μ_0 is the permeability of vacuum. Here the first and second terms on the right-hand side show the inductive and resistive flux consumption, respectively. The resistive flux consumption is calculated by the empirical Ejima formula for I_P ramp-up and from an approximated loop voltage formula for flat-top. However, the required $\Psi_{flat\text{-}top}$ is defined by:

$$\Psi_{flat\text{-}top} = V_{loop} t_{flat\text{-}top}, \tag{3}$$

where V_{loop} is the approximated loop voltage, and $t_{flat\text{-}top}$ is the operation time. The relationship that indicates the flux balance is given by:

$$\Psi_{Int} - \Psi_{op} = \Psi_{Link}, \tag{4}$$

where Ψ_{Int} and Ψ_{Link} are the initial exciting flux and the linked flux between the coils and the plasma, respectively. The Ψ_{Int} is constant, and the Ψ_{Link} is calculated by integrating the flux generated by the PF coil and conducting elements. Substituting Eqs. (2) and (3) into Eq. (4), Eq. (4) can be rewritten as:

$$\Psi_{Int} - \left(L_P I_P + C_{Ejima}\mu_0 R_P I_P + \Psi_{flat\text{-}top}\right) = \Psi_{Link}; \tag{5}$$

we then obtain:

$$\Psi_{flat\text{-}top} = \Psi_{Int} - \left(L_P I_P + C_{Ejima}\mu_0 R_P I_P + \Psi_{Link}\right). \tag{6}$$

The $\Psi_{flat\text{-}top\_input}$, which indicates the input value of the resistive flux for flat-top, is calculated using Eq. (3). Here, the I_P, in which the $\Psi_{flat\text{-}top}$ coincides with the $\Psi_{flat\text{-}top\_input}$, would be calculated by iteration. The correction of the I_P is given by:

$$dI_P = \frac{\left(\Psi_{flat\text{-}top} - \Psi_{flat\text{-}top\_input}\right)}{\left(L_P + C_{Ejima}\mu_0 R_P\right)}, \tag{7}$$

where dI_P is the correction of I_P. The iteration of Step 4 is done until the correction of I_P vanishes.

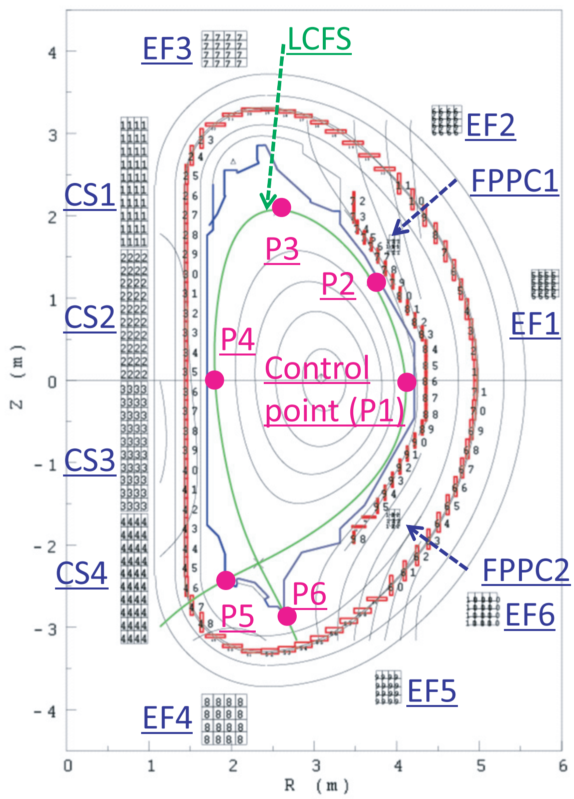

Fig. 2 Locations of the control points, the PF coils, in-vessel coils, and toroidal conducting elements in JT-60SA.

2.2 I_P control

The isoflux technique is used to control the position, shape, and I_P in JT-60SA. The set of locations that defines the desired plasma separatrix is specified as the control points. Figure 2 shows the locations of the control points, PF coils, in-vessel coils, and toroidal conducting elements in JT-60SA.

The PF coil currents are adjusted to maintain an equal poloidal flux at the control points for the control of plasma position and shape. The small difference between the flux at the control points and its reference value is defined as $\delta\boldsymbol{\Psi}_S$. The change in the coil currents required for the control of plasma position and shape is defined as $\mathrm{d}\boldsymbol{I}_{C,PS}$. The relationship between $\mathrm{d}\boldsymbol{I}_{C,PS}$ and $\delta\boldsymbol{\Psi}_S$ for the control of plasma position and shape can be represented as:

$$\mathrm{d}\boldsymbol{I}_{C,PS} = G_S \boldsymbol{M}^{-1}\{\delta\boldsymbol{\Psi}_S\}\,\mathrm{d}t, \tag{8}$$

where $\boldsymbol{M}^{-1}$ is the $(m \times (n+1))$ control matrix that is the generalized inverse of the Green function $\boldsymbol{M}$ calculated using the singular value decomposition method, and m and n are the number of PF coils and control points, respectively. The matrix $\boldsymbol{M}^{-1}$ is used not only to control position and shape but also for I_P control. The Green function $\boldsymbol{M}$ represents the poloidal flux at the X/limiter point and each control point per unit of current. It is necessary to include the component of the X/limiter point in the matrix because the controller changes the poloidal flux equally at the X/limiter point and control points for I_P control. G_S is the control gain of the position and shape feedback controls that are necessary to make the poloidal flux equal at all control points.

The $\delta\boldsymbol{\Psi}_S$ is defined as:

$$\{\delta\boldsymbol{\Psi}_S\} = \begin{pmatrix} 0 \\ \Psi_{surf} - \Psi_{P1} \\ \vdots \\ \Psi_{surf} - \Psi_{Pn} \end{pmatrix}, \tag{9}$$

where $\delta\boldsymbol{\Psi}_S$ is the $(n+1)$ vector of the difference between the reference flux value and the flux at the X/limiter point and control points, Ψ_{surf} is the flux at the plasma surface, and Ψ_{Pn} is the flux at the control point. It is necessary to include the component of the X/limiter point in $\delta\boldsymbol{\Psi}_S$ to multiply $\delta\boldsymbol{\Psi}_S$ by the matrix $\boldsymbol{M}^{-1}$. The first element is the difference at the the X/limiter point, and elements from the 2nd to the $(n+1)$ rows are difference at the control points. Thus, the 1st row of $\delta\boldsymbol{\Psi}_S$ is zero. The units of the variables are as follows: $\mathrm{d}I_C$ is in amperes, G_S is in s^{-1}, and Ψ_{surf} and Ψ_{Pn} are in webers.

However, the controller changes the poloidal flux equally at the X/limiter point and control points to reduce the difference between the actual value of I_P and its reference value without a change in the plasma position and shape for I_P control. The change in the poloidal flux required for I_P control is defined as $\mathrm{d}\Psi_{surf}$. The change in the coil currents required for I_P control is defined as $\mathrm{d}\boldsymbol{I}_{C,C}$. The relationship between $\mathrm{d}\boldsymbol{I}_{C,C}$ and $\mathrm{d}\Psi_{surf}$ for I_P control can be presented as:

$$\mathrm{d}\boldsymbol{I}_{C,C} = G_C \boldsymbol{M}^{-1}\{\boldsymbol{I}\}\mathrm{d}\Psi_{surf}, \tag{10}$$

where G_C is the control gain, and $\mathbf{I}$ is the $(n+1)$ vector in which all elements are 1. The $\mathrm{d}\Psi_{surf}$ would be provided by the PF coils in proportion to the difference between actual value of I_P and its reference value. Since the temporal differentiation of $\mathrm{d}\Psi_{surf}$ indicates the loop voltage, it can be presented as:

$$V_{loop} = -\frac{\mathrm{d}\Psi_{surf}}{\mathrm{d}t} = G_r\left(I_{P,ref} - I_P\right), \tag{11}$$

where $I_{P,ref}$ is the reference value of I_P, and G_r is the control gain. Therefore, Eq. (10) can be rewritten as:

$$\mathrm{d}\boldsymbol{I}_{C,C} = -G_C \boldsymbol{M}^{-1}\{\boldsymbol{I}\}G_r\mathrm{d}t(I_{P,ref} - I_P). \tag{12}$$

By defining G_X as $G_C G_r \mathrm{d}t$, Eq. (12) can be rewritten as:

$$\mathrm{d}\boldsymbol{I}_{C,C} = -G_X \boldsymbol{M}^{-1}\{\boldsymbol{I}\}(I_{P,ref} - I_P), \tag{13}$$

where G_X is the control gain of the I_P feedback controls that are necessary to change the poloidal flux equally at all control points. $G_r\mathrm{d}t$ is equal to L_P from the equation of magnetic energy balance at the plasma surface.

For the PF coils, proportional-integral (P-I) feedback control is used based on the sum of Eqs. (8) and (13) for the control of plasma position, shape, and I_P. The controller modifies the PF coil currents according to the following equation:

$$\boldsymbol{I}_{\mathrm{C}}(t+\Delta t) = \boldsymbol{I}_{\mathrm{C}}(t_0) + \boldsymbol{M}^{-1}\Big[G_{\mathrm{SP}}\{\delta\boldsymbol{\Psi}_{\mathrm{S}}(t)\} + G_{\mathrm{SI}}\int_{t_0}^{t}\{\delta\boldsymbol{\Psi}_{\mathrm{S}}(t)\}\mathrm{d}t - G_{\mathrm{XP}}\{\boldsymbol{I}\}(I_{\mathrm{P,ref}} - I_{\mathrm{P}}) - G_{\mathrm{XI}}\{\boldsymbol{I}\}\int_{t_0}^{t}\{I_{\mathrm{P,ref}} - I_{\mathrm{P}}\}\mathrm{d}t, \quad (14)$$

where t_0 is the initial time; Δt is the control cycle; G_{SP} and G_{SI} are the respective control gains of the P-I feedback controls that are necessary to make the poloidal flux equal at all control points; and G_{XP} and G_{XI} are the respective control gains of the P-I feedback controls necessary to change the poloidal flux equally at all control points. The units of the variables are as follows: G_{SP} and G_{XP} are dimensionless, and G_{SI} and G_{XI} are in s^{-1}. The values of G_{SP}, G_{XP}, G_{SI}, and G_{XI} are 1.0, 9.0, 1.0, and 10.0 in the following simulations, respectively.

3. Simulation Results

An operation scenario with I_{P} ramp-up and pressure increase is developed using the plasma equilibrium control simulator in JT-60SA. Equilibrium control capability against change in flux consumption is also to be discussed.

3.1 Study of the operation scenario during I_{P} ramp-up

The control of plasma position, shape, and I_{P} has been simulated during I_{P} ramp-up. The controlled plasma parameters are as follows: I_{P} increases from 1.0 to 5.5 MA, β_{P} increases from 0.10 to 0.74, and l_{i} decreases from 0.84 to 0.74. The reference values of I_{P}, β_{P}, and l_{i} changes during I_{P} ramp-up, and the I_{P} profile parameters are adjusted to fix the β_{P} and l_{i} to its reference value. All the equilibrium calculation cycles and control cycles of the PF coils and FPPC coils are 5 ms. Equilibrium control is simulated from t = 2.7 to 25.0 s. The initial controlled plasma is I_{P} = 1.0 MA, β_{P} = 0.10, and l_{i} = 0.84 with the limiter configuration. To make the transition from a limiter to a divertor configuration around t = 4.6 s, I_{P} is maintained from t = 3.9 to 4.6 s.

Figure 3 shows the waveforms of the plasma parameters and total eddy current flowing in the conducting elements during I_{P} ramp-up. The β_{P} and l_{i} are fixed to the reference values as shown in Fig. 3 (a). The actual value of I_{P} increases following the change in the reference value as shown in Fig. 3 (b). To do this, the poloidal flux at plasma surface and the linked flux increases (in the negative direction) during I_{P} ramp-up as shown in Fig. 3 (c). The total flux consumption calculated by the resistive and conductive consumption is in close agreement with the linked flux. The controller changes the poloidal flux equally at all control points, and the equilibrium calculation obtains the I_{P} with the flux consumption accurately. The total eddy current flowing in the conducting elements is about 80 kA

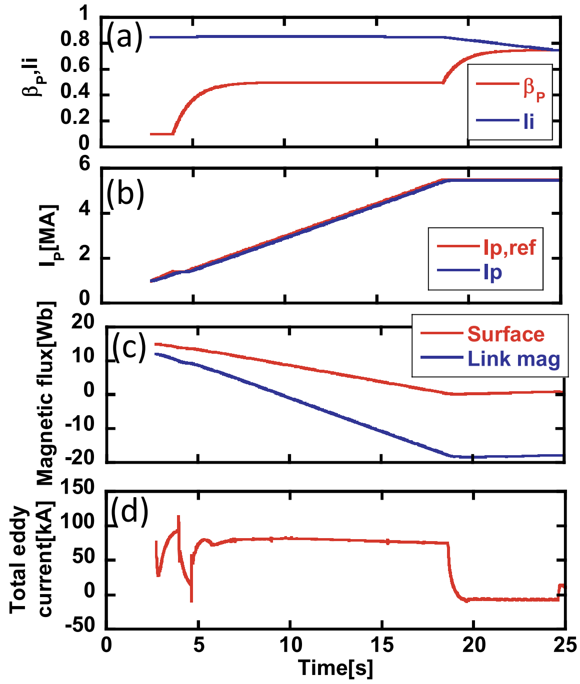

Fig. 3 Simulation results during I_{P} ramp-up. Waveforms of (a) the actual value of β_{P} and l_{i}, (b) the reference and actual values, (c) the flux at plasma surface and the linked flux between the plasma and coils, and (d) total eddy current flowing in the conducting elements.

during I_{P} ramp-up due to the change in I_{P} and PF coil currents. Figure 4 shows the equilibrium configurations at each time slice. The 6 initial input control points (P1 - P6) serves as the references for the plasma position and shape control at t = 2.7 s. The transition from a limiter to a divertor configuration is made in two steps: (1) an increase in the elongation, and (2) formation of the X point. Points P5 and P6 are moved in the horizontal and vertical directions, respectively, from t = 3.9 to 4.6 s. As a result, the elongation increases from approximately 1.58 to 1.73 as the plasma shape changed to follow the control points. Points P7 and P8 are added to specify the location of the strike points at t = 3.905 s. The divertor configuration is achieved by the formation of the X point at t = 4.6 s. The capability for the early formation of a divertor configuration is preferable. After the transition to the divertor configuration, the Points P1–P6 are operated to increase the plasma volume. Finally, the elongation and triangularity become approximately 1.79 and 0.50, respectively, at t = 24.6 s. Figure 5 shows the waveforms of the residual between the last closed flux surface (LCFS) and the control points, and PF coil currents. The residual in the positive direction indicates that the LCFS is outside the control point. The residual of P1, P2, and P6 initially increases by up to approximately 0.03 m due to an increase in both of the I_{P} and β_{P} as shown in Figs. 5 (a) and (b). The currents of EF1, EF2, and EF6 increases (in the negative direction) to reduce the residual of P1, P2, and P6, thus moving the

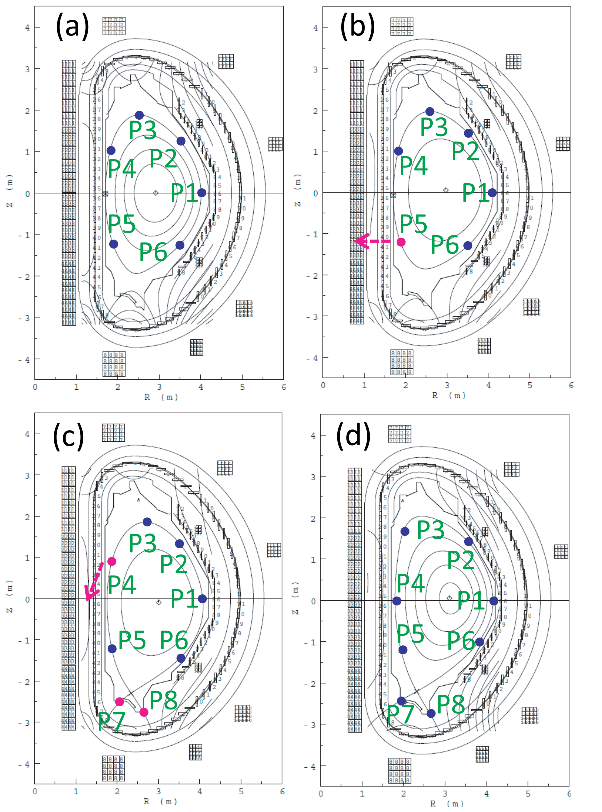

Fig. 4 Simulation results during I_P ramp-up. Equilibrium configurations (a) at $t = 2.7$ s, (b) 3.9 s, (c) 4.6 s, and (d) 24.6 s.

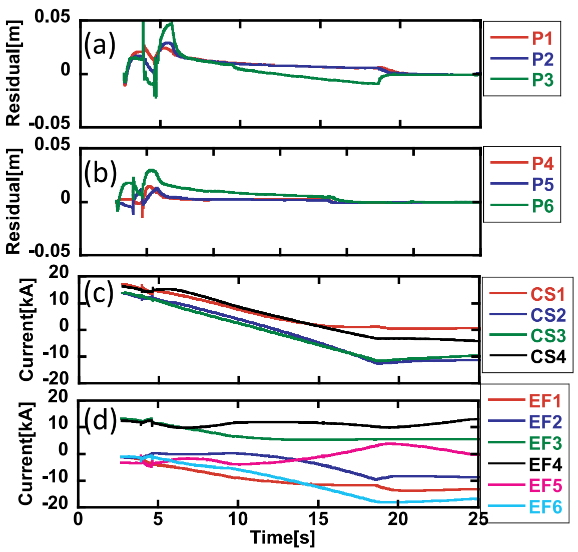

Fig. 5 Simulation results during I_P ramp-up. Waveforms of (a) residuals between P1-P3 and LCFS, (b) residuals between P4 - P6, (c) coil currents of CS1 - CS4, and (d) coil currents of EF1 - EF6.

outer plasma surface inward to the control points as shown in Fig. 5 (d). At the same time, the currents of CS1 - CS4 increased (in the negative direction) to change the poloidal flux equally at all control points for the I_P control as shown in Fig. 5 (c). Therefore, the simultaneous control of plasma position, shape, and I_P is achieved during I_P ramp-up.

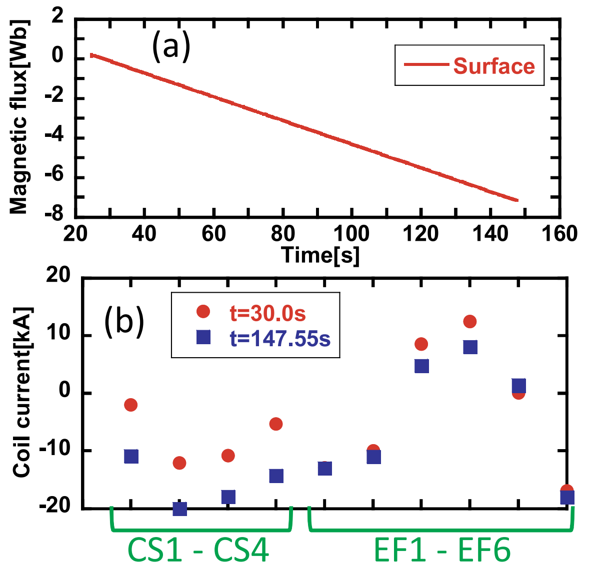

Fig. 6 Simulation results during I_P flat-top. Waveforms of (a) magnetic flux at the plasma surface and (b) coil currents of PF coils at $t = 30.0$ and 147.55 s.

3.2 Validation of the controllability of the LCFS during I_P flat-top

The control of plasma position, shape, and I_P has been simulated to validate the controllability of the LCFS during I_P flat-top. The PF coils need to keep changing the poloidal flux equally at all control points to maintain the I_P for the inductive operation. However, it is known how difficult it is to keep the desired plasma shape by maintaining I_P for a long time because changing the coil current of the finite length CS modules distorts the actual magnetic field around upper and lower sides of the plasma. The first example of validating the controllability of the LCFS is discussed with the change in PF coil currents for a long time. The controlled plasma parameters are as follows: $I_P = 5.5$ MA, $\beta_P = 0.74$, and $l_i = 0.74$ with the divertor configuration. All the equilibrium calculation cycles and the control cycles of the PF coils are 5 ms. The simulation should be performed until the PF coil achieves the limit of coil current in order to validate the controllability of the LCFS for as long as possible. The limit of PF coil currents are ± 20 kA. The 8 initial input control points (P1 - P8) serve as the references for the position and shape. The location of the control points are fixed at the initial location. Figure 6 show the waveforms of the poloidal flux at the plasma surface and the currents of PF coils. The currents of CS1 - CS4 increase (in the negative direction) to maintain the I_P for the inductive operation as shown in Fig. 6 (b). The current of CS2 reaches the limit of coil current at $t = 147.55$ s. The loop voltage is given as 0.06 V during I_P flat-top. The controller changes the poloidal flux by about 7.044 Wb from $t = 30.0$ to 147.55 s. The currents in EF3 and EF4 also decrease to reduce the residual

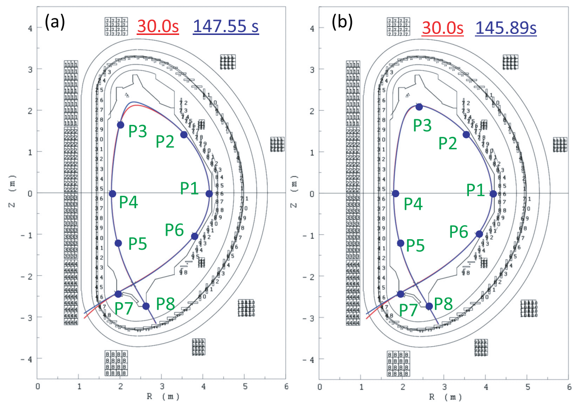

Fig. 7 Simulation results during I_P flat-top. (a) LCFS without optimizing the location of P3 at t = 30.0 (red solid line) and 147.55 s (blue solid line), and (b) LCFS with optimizing the location of P3 at t = 30.0 (red solid line) and 145.89 s (blue solid line).

induced by the change of the currents in CS1 and CS4. The effect of changing the current in PF coil on the controllability of the LCFS has been validated by the comparison of the LCFS at t = 30.0 s and the ending time when the limit of currents of CS coil is reached. Figure 7 (a) shows the comparison of the LCFS at t = 30.0 and 147.55 s. The location of the control points is fixed based on the above operation scenario during I_P ramp-up. Though the residual of the control points is almost zero, the difference in the LCFS around the upper and lower sides is observed over time. The location of Z_{top}, which is the top of the LCFS, increases from 2.117 to 2.196 m, and thus the elongation also increased from 1.827 to 1.864. The changing currents in the PF coils cause an unexpected change in the LCFS. This unexpected change in the LCFS has the potential to destabilize the control. To maintain the controllability of the LCFS during I_P flat-top, the location of the control point is optimized. Figure 7 (b) shows the comparison of the LCFS at t = 30.0 and 145.89 s. The location of control point P3 is optimized to control the LCFS during I_P flat-top. The difference in the LCFS decreases near the upper side, and thus the change in the location of Z_{top} and elongation are controlled. The location of control point also should be optimized to maintain the controllability of the LCFS during I_P flat-top.

4. Summary

A plasma equilibrium control simulator was developed for exploration of techniques to control plasma position, shape, and I_P. Functions to calculate and control the I_P with flux consumption were incorporated in the plasma position and shape control simulator. It is possible to simulate the control of the position, shape, and I_P and optimize the control logic in JT-60SA.

The control of plasma position, shape, and I_P has been simulated during I_P ramp-up. The actual value of I_P increased to follow the change in the reference value. The divertor configuration is achieved with the formation of an X point at the reference time by operating the control points. The simultaneous control of plasma position, shape, andI_P is achieved during I_P ramp-up.

The control of plasma position, shape, and I_P has been simulated to validate the controllability of the LCFS during I_P flat-top. The PF coil current needs to be changed continuously in order to control the poloidal flux equally at all control points to maintain the I_P for inductive operation. The change of currents in the PF coils causes an unexpected change in the LCFS. The location of control point also should be optimized to maintain the controllability of the LCFS during I_P flat-top.

In the future, the simulator will incorporate a coil voltage control scheme and plasma boundary identification code. Currently, the control points are manually adjusted to control the plasma position and shape. The new system will incorporate a control interface that will automatically adjust the number and location of control points in reference to the given plasma shape parameters such as elongation and triangularity. The controllability of the vertical instability will be validated using the simulator.

[1] S. Ishida *et al.*, Fusion Eng. Des. **85**, 2070 (2010).
[2] Y. Kamada *et al.*, Nucl. Fusion **51**, 073011 (2011).
[3] K. Tobita *et al.*, Fusion Eng. Des. **81**, 1151 (2006).
[4] K. Tobita *et al.*, Nucl. Fusion **49**, 075029 (2009).
[5] R.R. Khayrutdinov *et al.*, J. Comput. Phys. **107**, 106 (1993).
[6] K. Kurihara, Fusion Eng. Des. **51-52**, 1049 (2000).
[7] Y. Miyata *et al.*, Plasma Fusion Res. **7**, 1405137 (2012).
[8] F. Hofmann *et al.*, Nucl. Fusion **30**, 2013 (1990).